The environmental dependence of galaxy clustering in the Sloan Digital Sky Survey

Ummi Abbas[1]⋆ and Ravi K. Sheth[2]⋆

[1] *Department of Physics & Astronomy, University of Pittsburgh, Pittsburgh, PA 15260, USA*
[2] *Department of Physics & Astronomy, University of Pennsylvania, Philadelphia, PA 19104, USA*

5 February 2008

ABSTRACT
A generic prediction of hierarchical clustering models is that the mass function of dark haloes in dense regions in the Universe should be top-heavy. We provide a novel test of this prediction using a sample of galaxies drawn from the Sloan Digital Sky Survey. To perform the test, we compare measurements of galaxy clustering in dense and underdense regions. We find that galaxies in dense regions cluster significantly more strongly than those in less dense regions. This is true over the entire 0.1–30 Mpc pair separation range for which we can make accurate measurements. We make similar measurements in realistic mock catalogs in which the only environmental effects are those which arise from the predicted correlation between halo mass and environment. We also provide an analytic halo-model based calculation of the effect. Both the mock catalogs and the analytic calculation provide rather good descriptions of the SDSS measurements. Thus, our results provide strong support for hierarchical models. They suggest that, unless care is taken to study galaxies at fixed mass, correlations between galaxy properties and the surrounding environment are almost entirely due to more fundamental correlations between galaxy properties and host halo mass, and between halo mass and environment.

Key words: methods: analytical - galaxies: formation - galaxies: haloes - dark matter - large scale structure of the universe

1 INTRODUCTION

The correlation between galaxy properties (morphology, star formation rates, luminosity, color etc.) and the surrounding environment has been the subject of extensive studies in the last few decades: dense environments are preferentially occupied by elliptical, red, luminous galaxies, whereas star formation rates are higher in less dense regions (Dressler 1980; Butcher & Oemler 1984; Norberg et al. 2001, 2002; Balogh et al. 2002; Gomez et al. 2003; Hogg et al. 2004; Kauffmann et al. 2004; Berlind et al. 2005; Croton et al. 2005). In hierarchical models, this behaviour is expected to be a consequence of the fact that galaxies are surrounded by dark matter halos, and the properties of halos (mass, formation time, concentration, internal angular momentum, etc.) are correlated with their environments (Mo & White 1996; Sheth & Tormen 1999, 2002, 2004; Lemson & Kauffmann 1999; Gottloeber et al. 2001; Avila-Reese et al. 2005; Gao et al. 2005; Harker et al. 2006; Wechsler et al. 2006).

⋆ E-mail: ummi@phyast.pitt.edu (UA); shethrk@physics.upenn.edu (RKS)

Recently, we described how the clustering of galaxies can be used to test the assumption that the correlations between galaxy properties and their environments are *entirely* a consequence of the correlations between haloes and their environments (Abbas & Sheth 2005). This is a strong assumption which significantly simplifies interpretation of the observed luminosity dependence of galaxy clustering (e.g. Zehavi et al. 2005). It is also a standard assumption in current halo-model descriptions of galaxy clustering (see Cooray & Sheth 2002 for a review). The main goal of this paper is to perform this test.

This paper is arranged as follows: in Section 2 we show how galaxy clustering depends on environment in the SDSS (Adelman-McCarthy et al. 2006). In particular, we measure the pair correlation function in redshift space, $\xi(s|\delta_s)$, for a range of environments δ_s, as well as the projected quantity, $w_p(r_p|\delta_s)$; the latter is free of redshift-space distortions. These measurements are compared with similar measurements in carefully constructed mock catalogs, and from an analytic calculation based on the halo-model. In both the mocks and the analytic calculation, correlations between galaxy properties and environment are entirely a consequence of the correlation between galaxy properties and halo

masses, and between halo mass and environment. We summarize our results in Section 3, where we also discuss some implications. An Appendix provides details of the analytical model, which generalizes our earlier (real-space) work so that it can be used to model redshift space measurements as well.

2   THE ENVIRONMENTAL DEPENDENCE OF CLUSTERING

To measure the environmental dependence of clustering, we must decide on a measure of the environment. Abbas & Sheth (2005) showed that the precise choice of environment is not particularly important, in the sense that different choices lead to quantitative but not qualitative differences. They used N_R, the number of galaxies in a sphere of radius R centred on a galaxy, as a measure of that galaxy's environment, and presented results for $R = 5$ and $8h^{-1}$Mpc. Their analysis was performed in real-space. Performing a similar analysis in redshift-space is complicated because the environmental effect we would like to test is due to correlations between halo masses with the real-space density. Therefore, we must find a definition of density in redshift space which is as faithful as possible to that in real-space.

Line-of-sight redshift-space distortions can make a sphere in real-space appear very different in redshift space. For instance, around a spherically symmetric cluster there are two main effects: one is due to coherent infall around the center of the cluster, which appears as a squashing effect along the line of sight in redshift space (Kaiser 1987). The second is the "finger of God" effect which is due to the virial motions of galaxies within the cluster (de Lapparent et al. 1986). This shows up as an elongation of the cluster along the line of sight. The squashing effect is relatively small, producing effects of order unity or less, whereas the finger-of-god distortions are more dramatic—elongations along the line of sight are typically about a factor of ten. Since clusters have radii of a Mpc or so, fingers of god can extend up to about 10 Mpc. Therefore, while counts in redshift space spheres of radii $5h^{-1}$Mpc are not expected to faithfully trace the counts in the corresponding real-space spheres, counts in spheres of radii $8h^{-1}$Mpc, N_8 should be more similar. For this reason, in what follows we use N_8 as a measure of the environment of each galaxy. (If we wished to push to smaller scales, we could identify all the fingers of god, and then "decompress" them, by rescaling the distances along the line-of-sight so that they have the same extent as across the line-of-sight e.g. Tegmark et al. 2004. But performing such a "manicure" is beyond the scope of the present work.)

We use N_8 to divide the galaxy population into three equal-sized subsamples: the third with the largest values of N_8 are defined as being the dense subsample, and the third with the smallest values of N_8 are the underdense subsample. We then measure the correlation functions in these two subsamples.

Our strategy is to make such measurements in a volume limited galaxy catalog, so that selection effects are minimized. We then compare with similar measurements in realistic mock catalogs. Throughout, we show results for a flat ΛCDM model for which $(\Omega_0, h, \sigma_8) = (0.3, 0.7, 0.9)$ at $z = 0$. Here Ω_0 is the density in units of critical density today, the
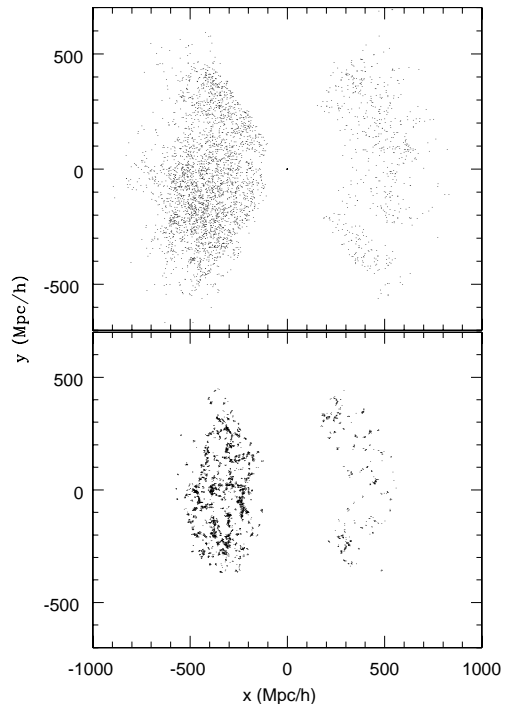

Figure 1. Pie-diagrams of the SDSS subsamples: top and bottom panels show the distributions of objects classified as being in the least dense and the densest regions, in a slice of thickness $100 \ h^{-1}$Mpc through the survey volume.

Hubble constant at the present time is $H_0 = 100h$ km s^{-1} Mpc^{-1}, and σ_8 describes the rms fluctuations of the initial field, evolved to the present time using linear theory, when smoothed with a tophat filter of radius $8h^{-1}$ Mpc.

2.1   The SDSS galaxy sample

We perform our analysis on a volume limited catalog extracted from the SDSS DR4 database (Adelman-McCarthy et al. 2006). We chose galaxies brighter than $M_r < -21$, to match the analysis of Zehavi et al. (2005), whose results we use below. The resulting catalog contains about 75000 objects with accurate angular positions and redshifts, where the number density is $0.00117 \ (h^{-1}$Mpc$)^{-3}$.

As discussed above, we define the environment of each object using the redshift-space information. Figure 1 shows the spatial distribution of galaxies in a thin slice through the SDSS volume limited catalog. Top panel shows the objects classified as being in the least dense regions, and bottom panel are for the objects in the densest regions. The galaxies in dense regions are clearly strongly clustered on small scales, whereas those in the underdense regions populate the holes defined by the spaces between the clusters that one sees in the dense sample.

The following sections quantify these differences by measuring the correlation functions in these subsamples. Uncertainties on our measurements were estimated by jackknife resampling, in which the statistics were remeasured after omitting a random region, and repeated thirty times

(approximately 1.5 times the total number of bins in separation for the results presented).

2.2 Mock galaxy samples

We have generated realistic mock galaxy samples as follows. We start with the Very Large Simulation (VLS; Yoshida, Sheth & Diaferio 2001), kindly made available to the public by the Virgo consortium. It has 512^3 particles in a cubic box with sides $L = 479h^{-1}$Mpc. About 800,000 dark matter halos, each containing at least 10 particles, were identified in this particle distribution using the Friends-of-Friends method. We use the simulation output for the mass, position and velocity of each dark matter halo.

   We use the results of Zehavi et al. (2005) to motivate our choice for how mock galaxies should be distributed within each halo. Specifically, to model a volume limited galaxy catalog with objects more luminous than L, halos less massive than m_L are assumed to contain no galaxies; m_L depends on the galaxy population under consideration. Galaxies more massive than m_L, contain one central galaxy, and may also contain satellite galaxies. The number of satellites is drawn from a Poisson distribution with mean $\langle N_s|m\rangle$, where

$$\langle N_s|m\rangle = \left(\frac{m}{m_1}\right)^\alpha \qquad \text{if } m \geq m_L. \qquad (1)$$

For SDSS galaxies more luminous than $M_r < -21$, $m_L = 10^{12.72}h^{-1}M_\odot$, $m_1 = 23m_L$, and, $\alpha = 1.39$ (Zehavi et al. 2005). (A Poisson distribution for the number of satellites is motivated by the work of Kravtsov et al. 2004). We then assume that the satellites in a halo are distributed around the halo center similarly to the dark matter (e.g. Navarro et al. 1997).

   To model redshift space effects, we must model the velocity vector of each mock galaxy. We do so by assuming that $v_{\rm gal} = v_{\rm halo} + v_{\rm vir}$, where $v_{\rm halo}$ is the halo motion provided by the simulation, and $v_{\rm vir}$ is obtained as follows. The central galaxy in a halo is assumed to be at rest with respect to the halo, so $v_{vir} = 0$. The virial motions of satellite galaxies are modelled by assuming that haloes are isotropic, virialized, and isothermal with Maxwellian velocities around the halo center. The one-dimensional velocity dispersion is $1000\,(r_{200}h/{\rm Mpc})/\sqrt{2}$, where r_{200} is the scale on which the enclosed mass is 200 times the critical density: $m = 200\bar\rho_{\rm crit}\,(4\pi r_{200}^3/3)$. Following results in Sheth & Diaferio (2001), we assume that this virial term is independent of local environment.

   In the distant observer approximation, the position in redshift space is $s = x + v_x/H_0$, where x is the real-space coordinate in the x-direction, v_x is the x-component of the peculiar velocity. and s is the redshift-space distance in the x-direction. The y- and z- components of the position are unchanged. The isothermal Maxwellian assumption means that the virial motions add Gaussian noise to the line-of-sight position of each satellite galaxy.

   We then measure N_8 for each galaxy by counting the total number of galaxies within $8h^{-1}$Mpc. For the mock catalog, we can do this in both real- and redshift-space. Figure 2 compares these two estimates of the local density. They are not widely different, suggesting that the analysis in the Appendix will be useful.
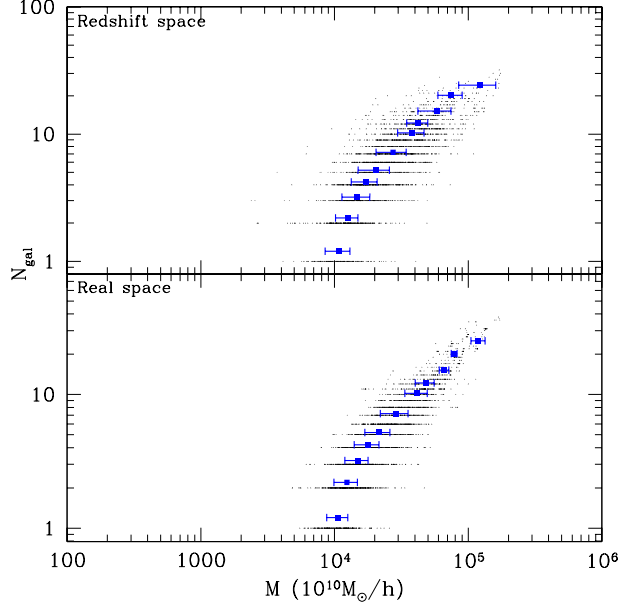

Figure 2. Comparison of local density estimates within real (bottom) and redshift (top) space spheres of radius $8h^{-1}$Mpc. The median (given by the squares) and quartile range of halo mass corresponding to certain number of galaxies is shown (for clarity these points have been shifted upwards).

2.3 Results

Figure 3 quantifies the spatial differences seen in Figure 1; it shows the redshift space correlation functions in dense and underdense regions measured in the mock catalogs (upper panel) and in the SDSS volume limited catalog (lower panel). In both panels, $\xi(s|\delta_s)$ for the dense sample is significantly larger than it is in the underdense sample. On large scales, this is because dense regions host the most massive haloes which in turn contain many galaxies; on smaller scales, the fact that the halo density profiles depend on halo mass also matters (Abbas & Sheth 2005). The inflection or break at the scale on which we define the environment ($8h^{-1}$ Mpc), which is seen in the clustering signal for underdense regions, arises because this scale is significantly larger than the virial radius of a typical halo. Let R denote the scale on which the environment is defined. Then, pairs which come from different halos are of two types: those separated by scales smaller than R are said to be in the same patch, whereas more widely separated pairs are in different patches. Abbas & Sheth (2005) called these the $2h - 1p$ and $2h - 2p$ contributions to the statistic. Now, by definition, there are no $2h - 2p$ pairs with separations smaller than $8h^{-1}$ Mpc, so $\xi_{2h-2p} = -1$ on smaller scales. In addition, underdense regions are those with small N_R, so they have few pairs in the $2h-1p$ term by definition. In the limit in which there is only one halo in each underdense patch (i.e., the one surrounding the galaxy around which the patch was centered), there will be no $2h - 1p$ pairs. In this limit, the correlation function is the sum of the 1h term, which falls rapidly on scales larger than the virial radius (a few Mpc) and the $2h - 2p$ term (which is only significant on scales larger than the patch radius). Therefore, in this limit, if R is significantly larger
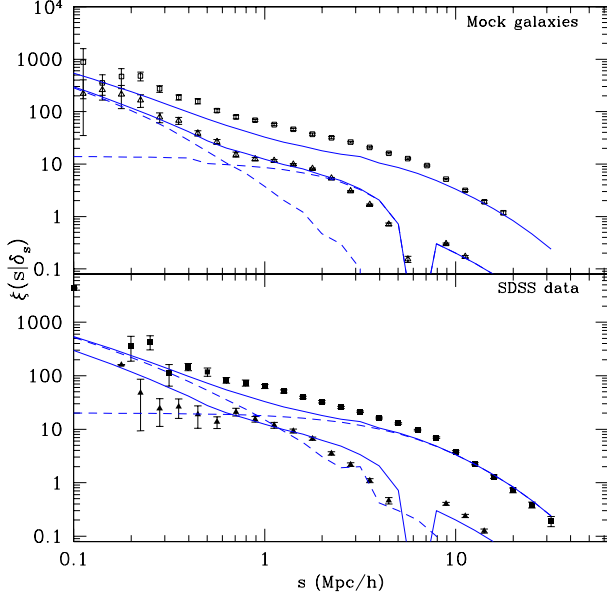
Figure 3. Environmental dependence of the galaxy correlation function in redshift space. Upper panel shows measurements in the mock catalog, and lower panel shows measurements in the SDSS. In both cases, the galaxy catalog is volume limited to $M_r < -21$, and the environment of a galaxy was defined by counting the number of galaxies within a redshift-space sphere of radius $8h^{-1}$Mpc centred on it. The squares and triangles in each panel show $\xi(s|\delta_s)$ for the galaxies in the densest 1/3 and least dense 1/3 of the sample. Solid curves show the analytic model for $\xi(s|\delta_s)$ that is developed in Appendix A. Dashed curves in the upper panel show the 1-halo (dominates on small scales) and the sum of the 2h-1p and 2h-2p contributions (dominate on intermediate and large scales, respectively) to $\xi(s|\delta_s)$ of the less-dense sample. In the lower panel, the dashed curves show these contributions for the dense sample.

than the virial radius of a typical halo, there will be a dramatic feature in ξ at scale R. As the number of $2h - 1p$ pairs increases, this feature becomes less obvious. Indeed, in dense regions—those which have larger N_R and so have more $2h - 1p$ pairs, there is little evidence of this feature.

The solid curves in the two panels show the analytic calculation outlined in the Appendix. They provide a reasonable description of the measurements in both panels. However, while the agreement is good on large scales, the curves underestimate the small-scale signal in dense regions. Since these smaller scales are the ones most affected by finger-of-god distortions, it may be that the discrepancy is due to inadequacies in the analytic treatment of redshift-space effects (see Scoccimarro 2004 for a discussion of the sorts of effects our analysis ignores).

To eliminate this source of uncertainty, we have also studied the projected quantity

$$w_p(r_p|\delta_s) = 2 \int_0^\infty d\pi\, \xi(r_p, \pi|\delta_s); \qquad (2)$$

where $r = \sqrt{r_p^2 + \pi^2}$. We integrate up to $\pi = 35\ h^{-1}$Mpc, which is large enough to include most correlated pairs. Figure 4 shows the results, both in the mock catalog (top panel) and in the SDSS (bottom panel). Now, the agreement with
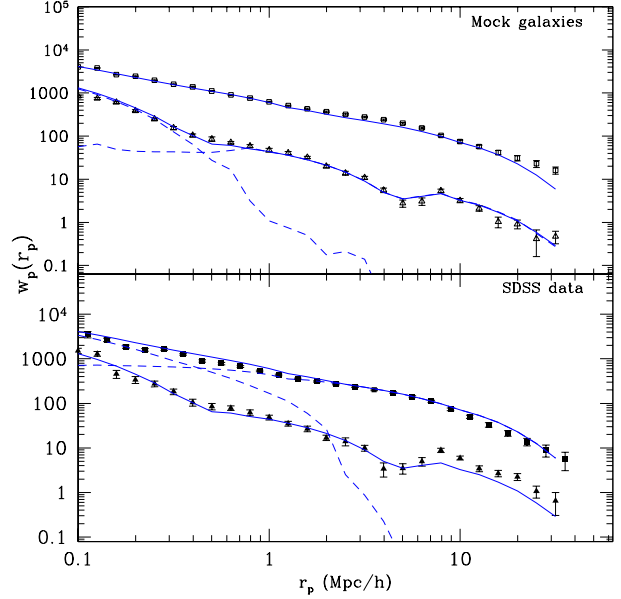
Figure 4. Similar to Figure 3, but now for the projected galaxy correlation function. The upper panel shows measurements in the mock catalog, and the lower panel is for the SDSS. Symbols and line-styles are the same as for Figure 3.

the analytical model is very good, suggesting that our analytic treatment of redshift-space distortions is inadequate. Once again, the inflection at the scale of the patch size for the underdense sample is caused due to the transition from one type of 2-halo term to the other.

Both for $\xi(s|\delta_s)$ and $w_p(r_p|\delta_s)$ the differences between the two environments are dramatic—they are measured with high statistical significance. Nevertheless, the analytic model, which only incorporates those correlations with environment which arise from the correlation between halo mass and environment, provides an excellent description of the measurements. This leaves little room for other environmental effects.

3   DISCUSSION AND CONCLUSIONS

One of the luxuries of the latest generation of large-scale sky surveys is that they contain sufficiently many objects that one can study subsamples of galaxies divided up in various ways. Here, we have focused on the clustering of galaxies in a volume limited sample drawn from the SDSS, and studied how the clustering of these galaxies depends on environment. We find that galaxies in dense regions are considerably more strongly clustered than those in less dense regions (Figures 3 and 4).

This is perhaps not so surprising—after all, a dense region is one in which many galaxies are crowded together. What is more surprising is that this dependence on environment is very well reproduced by numerical (Section 2.2) and analytic (Appendix A) models in which the entire effect is due to the fact that galaxy properties correlate with the masses of their parent halos, and massive halos preferentially populate dense regions. Hierarchical models make quantita-

tive predictions for this correlation between halo mass and environment, and so the agreement between our models and the measurements provides strong support for such models. In this respect, our results are consistent with those of Mo et al. (2004), Kauffmann et al. (2004), Berlind et al. (2005), Blanton et al. (2006) and Skibba et al. (2006); this is reassuring, since our methods are very different.

Our test of environmental effects is particularly interesting in view of recent work showing that, at fixed mass, haloes in dense regions form earlier (Sheth & Tormen 2004), and that this effect is stronger for low mass haloes (Gao et al. 2005; Harker et al. 2006; Wechsler et al. 2006). Such a correlation is not part of our analytic model, nor is it included in our mock catalogs. Presumably, the good agreement with the SDSS measurements is due to the fact that we have concentrated on luminous galaxies, and these populate the more massive haloes. It will be interesting to see if this agreement persists at lower luminosities.

The agreement between our models and the measurements has an important consequence: Unless care is taken to study a population at fixed halo mass, our results indicate that observed correlations between gastrophysical effects (e.g. ram pressure stripping, strangulation, harrassment) and environment are dominated by the fact that these effects also correlate with halo mass, and halo mass correlates with environment.

Larger samples will allow us to study if these trends persist to fainter, presumably less massive galaxies. And more distant samples will allow us to study if these trends evolve.

REFERENCES

Abbas U., Sheth R.K., 2005, MNRAS, 364, 1327
Adelman-McCarthy J.K. et al., 2006, ApJS, 162, 38
Avila-Reese V., Colin P., Gottloeber S., Firmani C., Maulbetsch C., 2005, ApJ, 634, 51
Balogh M.L., Bower R.G., Smail I., Ziegler B.L., Davies R.L., Gaztelu A., Fritz A., 2002, MNRAS, 337, 256
Berlind A.A., Blanton M.R., Hogg D.W., Weinberg D.H., Dave R., Eisenstein D.J., Katz N., 2005, ApJ, 629, 625
Blanton M.R., Eisenstein D.J., Hogg D.W., Zehavi I., 2004, ApJ, 645, 977
Butcher H., Oemler A., 1984, ApJ, 285, 426
Croton D.J., et al., 2005, MNRAS, 356, 1155
Cooray A., Sheth R.K., 2002, Phys. Rep., 372, 1
Davis M., Peebles P.J.E., 1983, ApJ, 267, 465
de Lapparent V., Geller M.J., Huchra J.P., 1986, ApJ, 302, L1
Dressler A., 1980, ApJ, 236, 351
Gao L., Springel V., White S. D. M., 2005, MNRAS, 363, L66
Gomez P.L. et al., 2003, ApJ, 584, 210
Gottloeber S., Klypin A., Kravtsov A.V., 2001, ApJ, 546, 223
Harker G., Cole S., Helly J., Frenk C., Jenkins A., 2005, MNRAS, 367, 1039
Hogg D.W. et al., 2004, ApJ, 601, L29
Kaiser N., 1987, MNRAS, 227, 1
Kauffmann G. et al., 2004, MNRAS, 353, 713
Kravtsov A.,Berlind A.A., Wechsler R.H., Klypin A.A., Gottloeber S., Allgood D.B., Primack J.R., 2004, ApJ, 609, 35
Lemson G., Kauffmann G., 1999, MNRAS, 302, 111
Mo H.J., White S.D.M., 1996, MNRAS, 282, 347
Mo H. J., Yang X., van den Bosch F. C., Jing Y. P., 2004, MNRAS, 349, 205
Navarro J.F., Frenk C.S., White S.D.M., 1997, ApJ, 490, 493
Norberg P. et al., 2001, MNRAS, 328,64
Norberg P. et al., 2002, MNRAS, 332,827
Scoccimarro R., 2004, PhRvD, 70. 3007
Seljak U., 2001, MNRAS, 325, 1359
Sheth R.K., 1996, MNRAS, 279, 1310
Sheth R.K., 1998, MNRAS, 300, 105
Sheth R.K., Diaferio A., 2001, MNRAS, 322, 901
Sheth R.K., Tormen G., 1999, MNRAS, 308, 119
Sheth R.K., Tormen G., 2002, MNRAS, 329, 61
Sheth R.K., Tormen G., 2004, MNRAS, 350, 1385
Skibba R., Sheth R.K., Connolly A.J., Scranton R., 2006, MNRAS, 368, 68
Tegmark M., et al., 2004, ApJ, 606, 702
Wechsler R.H., Zentner A.R., Bullock J.S., Kravtsov A.V., 2005, ApJ submitted (astro-ph/0512416)
White M., 2001, MNRAS, 321, 1
Yoshida N., Sheth R.K., Diaferio A., 2001, MNRAS, 328, 669
Zehavi I. et al., 2005, ApJ, 630, 1

APPENDIX A: THE ANALYTICAL MODEL

This Appendix discusses how the halo model calculation of environmental effects on clustering can be extended to include redshift-space effects. Our strategy is to combine the halo-model description of redshift space effects (White 2001; Seljak 2001) with the halo model description of environmental effects provided by Abbas & Sheth (2005).

In redshift space, two effects modify the real space expressions derived by Abbas & Sheth (2005). One of these is a boost of power on large scales due to the instreaming of matter into overdense regions (Kaiser 1987); this affects the 2-halo terms. Using density conservation to linear order and making the distant observer approximation, the

redshift-space galaxy density perturbation can be written as

$$\delta_g^{rs} = \delta_g + \delta_v \mu^2 \qquad (A1)$$

where $\mu = \hat{r} \cdot \hat{k}$, δ_g is the real space galaxy density perturbation and δ_v is the velocity divergence. This is related to the density perturbation δ_{dm} via $\delta_v = f\delta_{dm}$, where $f(\Omega) \equiv d\log\delta/d\log a \simeq \Omega^{0.6}$, and a is the scale factor.

The other effect is the suppression of power due to the virial motions within haloes; this affects the 1-halo term (Sheth 1996). The assumption of isotropic, isothermal, Maxwellian motions within halos means that the effect can be modeled as a convolution with a Gaussian. In particular, the density contrast in redshift space is

$$\delta_g^{rs} = \delta_g e^{-(k\sigma\mu)^2/2}. \qquad (A2)$$

Scoccimarro (2004) discusses why these descriptions (equations A1 and A2) of redshift-space distortions are rather crude. For our purposes, they represent reasonable first approximations to a more sophisticated model.

Let $n(M,V)$ denote the number density of patches of mass M and volume V, and let $N(m|M,V)$ be the average number of m haloes in regions of volume V which contain mass M. The isotropized redshift space power spectrum is obtained by averaging $(\delta_g^{rs})^2$ over μ, m and M. In particular, the 1-halo term can be written as,

$$P_{1h}^{gal}(k|\delta) = \int_{M_{min}}^{M_{max}} dM\, n(M,V) \int_0^M dm\, N(m|M,V)$$
$$\times \frac{[\langle 2N_s|m\rangle\, u(k|m)\Re_1(k\sigma) + \langle N_s|m\rangle^2\, |u(k|m)|^2 \Re_2(k\sigma)]}{\bar{n}_{\delta-gal}^2}, \qquad (A3)$$

where

$$\Re_p(\alpha = k\sigma[p/2]^{1/2}) = \frac{\sqrt{\pi}}{2}\frac{\mathrm{erf}(\alpha)}{\alpha} \qquad (A4)$$

for $p = 1, 2$, and $\bar{n}_{\delta-gal}$ is the number density of galaxies surrounded by regions containing at least N_{min} other galaxies:

$$\bar{n}_{\delta-gal} = \int_{M_{min}(N_{min})}^{M_{max}(N_{max})} dM\, n(M,V)$$
$$\times \int_0^M dm\, N(m|M,V)\,\langle N_{gal}|m\rangle. \qquad (A5)$$

Here, $\langle N_{gal}|m\rangle = 1+\langle N_s|m\rangle$ is the average number of galaxies occupying a halo of mass m (in our model, it is zero below some m_L; c.f. equation 1). In practice, $M_{min}(N_{min})$ is obtained by varying N_{min} until the value of this expression matches the observed number density.

The two-halo term is more complex as it now has two types of contributions: pairs which are in the same patch (2h-1p), and pairs in different patches (2h-2p). The 2h-1p term can only be important on intermediate scales (i.e., those which are larger than the diameter of a typical halo but smaller than the diameter of a patch). The 2h-2p term is

$$P_{2h-2p}^{gal} = (F_g^2 + \frac{2}{3}F_v F_g + \frac{1}{5}F_v^2)P_{\mathrm{Lin}}(k|R_p), \qquad (A6)$$

where

$$F_v = f\int_{M_{min}}^{M_{max}} dM\, n(M,V)\, B(M,V)$$
$$\times \int_0^M dm\, N(m|M,V)\frac{m}{\rho_\delta}\Re_1(k\sigma)u(k|m)$$
$$F_g = \int_{M_{min}}^{M_{max}} dM\, n(M,V)\, B(M,V) \qquad (A7)$$
$$\times \int_0^M dm\, N(m|M,V)\frac{\langle N_{gal}|m\rangle}{\bar{n}_{\delta-gal}}\Re_1(k\sigma)u(k|m);$$

$P_{\mathrm{Lin}}(k|R_p)$ denotes the power spectrum associated with setting the linear theory correlation function to -1 on scales smaller than the diameter of a patch $2R_p$. This truncation has little effect on small $kR_p \ll 1$, where $P_{\mathrm{Lin}}(k|R_p) \approx P_{\mathrm{Lin}}(k)$. And the factor $B(M,V)$ describes the bias associated with the clustering of the patches; it depends on the abundance of such patches (see Abbas & Sheth 2005 for details).

Similarly, the 2h-1p term can be written as

$$P_{2h-1p}^{gal}(k|\delta) = \int_{M_{min}}^{M_{max}} dM\, n(M,V)(F_g^{'2} + \frac{2}{3}F_v' F_g' + \frac{1}{5}F_v^{'2})$$
$$\times \Big[P_{Lin}(k) - P_{Lin}(k|R_p)\Big], \qquad (A8)$$

where $P_{\mathrm{Lin}}(k) - P_{Lin}(k|R_p)$ denotes the power spectrum associated with setting the linear theory correlation function to zero on scales larger than the diameter of a patch $2R_p$, and

$$F_v' = f\int_0^M dm\, N(m|M,V)\frac{m}{\rho_\delta}\Re_1(k\sigma)b(m)\, u(k|m)$$
$$F_g' = \int_0^M dm\, N(m|M,V)\frac{\langle N_{gal}|m\rangle}{\bar{n}_{\delta-gal}}\Re_1(k\sigma)b(m)\, u(k|m). \qquad (A9)$$

Here $b(m)$ is the bias factor of haloes of mass m (from Sheth & Tormen 1999). The correlation function, $\xi(s)$, is obtained by taking the Fourier transform of the power spectrum $P(k)$.